STRUCTURAL CONTROL AND HEALTH MONITORING
Struct. Control Health Monit. (2012)
Published online in Wiley Online Library (wileyonlinelibrary.com). DOI: 10.1002/stc.1502

Optimal design of an array of active tuned mass dampers for wind-exposed high-rise buildings

Ilaria Venanzi*,†, Filippo Ubertini and Annibale Luigi Materazzi

University of Perugia, Perugia, Italy

ABSTRACT

In this paper, a comprehensive procedure is developed for the optimization of a hybrid control system for tall buildings subjected to wind-induced vibrations. The control system is made of active tuned mass dampers (ATMDs) and is conceived to mitigate the flexural and torsional response in serviceability limit state conditions. The feedback information necessary to compute the control forces is provided by a limited number of accelerometers arranged over the building's height. To reduce the computational effort, subsequent optimization subprocedures are employed that take advantage of the genetic algorithm to find the solution of the nonlinear, constrained optimization problems. At first, the optimization of the ATMDs' number and positions over the top floor of the building is carried out. Then, the optimal location of the accelerometers over the building's height is obtained. The reduction of the flexural and torsional accelerations is chosen as target of the optimization problem. The technical limitations of the ATMDs, such as the actuators saturation and the limited stroke extensions, are the constraints to the problem. As an illustrative example, a control system is optimized for the response mitigation of a tall building subjected to wind load. Copyright © 2012 John Wiley & Sons, Ltd.

Received 12 October 2011; Revised 3 April 2012; Accepted 15 April 2012

KEY WORDS: hybrid control system, optimal design, tall buildings, wind-excited vibrations, translational and torsional response

1. INTRODUCTION

The current trend of constructing taller and sometimes nonsymmetric buildings implies the need to control both flexural and torsional vibrations induced by wind. In order to satisfy serviceability limits, many high-rise buildings are equipped with passive, semi-active, or hybrid control systems [1]. The most common ones are passive devices, such as tuned mass dampers (TMDs) [2,3], that do not require power supply. However, these systems are well known to be subjected to frequency mistuning, which might strongly weaken their effectiveness in practical applications. Multiple TMDs (MTMDs) and smart TMDs can partially circumvent this drawback, but their application in tall buildings is not free from a degree of complexity [4–11]. An effective approach, which has already been used in a number of applications, is to use hybrid control systems, such as active tuned mass dampers (ATMDs), which share the advantages of the active control, needing a lower actuation power with respect to the purely active systems, with the capability of working as passive systems when power supply is missing [12,13]. Investigations on the optimal control performance and design methods of an ATMD system in order to achieve satisfactory control effectiveness have nowadays been carried out, for example, by Yan *et al.* [14], Ahlawat and Ramaswamy [15], and Li *et al.* [16]. A possible development is using an array of MTMDs, the so called

*Correspondence to: Ilaria Venanzi, Department of Civil and Environmental Engineering, University of Perugia, Via G. Duranti 93, 06125 Perugia, Italy.
†E-mail: ilaria.venanzi@strutture.unipg.it

active MTMDs (AMTMDs), which have the advantage to subdivide the large control force into many smaller control forces without losing the level of response reduction [17,18].

The design of such complex devices involves many aspects.

The first issue is the optimal calibration of the characteristics of the tuned masses, such as stiffness, damping, and their position especially in the case of irregular buildings. The topic has been widely studied [19], but there are still some aspects that deserve investigation [20–22].

Moreover, the role of physical limits such as actuators saturations and limited stroke extensions of inertial actuators must be properly taken into account. This issue was considered for example in [23], where a nonlinear control strategy for application against earthquake excitation that accounts for physical limitations directly in the control law was proposed.

In a general framework of limited resources, another issue for the design of the control system is the optimal choice of the number and location of actuators and sensors [24]. As the current trend is constructing more flexible and irregular buildings, with a 3D coupled response under the external excitation, the need to find the optimal position of actuators and sensors becomes more and more important [16].

In this paper, a comprehensive methodology for the optimal design of a hybrid control system made of arrays of ATMDs for the flexural/torsional response mitigation of tall buildings is proposed. Using subsequent optimization subprocedures, the number and position of the ATMDs and the sensors' locations are optimized. The minimization of the flexural and torsional accelerations is chosen as target of the optimization problem. The technical limits of the ATMDs, such as the actuators saturation and the limited stroke extensions, are considered as constraints to the problem. This approach specifically conceived for serviceability conditions (in case of extreme loads, an emergency stop will save the actuators) results in a less demanding control strategy with respect to the one presented in [23]. Another major advantage of this approach is that it does not require approximations on the characteristics of the wind-induced actions and of the dynamic system under investigation and provides automatically the optimal design of all the components of the control system. The application to a case study shows that the method is effective and capable to achieve the result with a reasonable computational effort.

2. FORMULATION OF THE CONTROL ALGORITHM

The hybrid control system considered in this paper is made of an array of ATMDs located at the top floor of a tall building. The structure is schematized considering three DOFs for each floor. The total number of DOFs of the system is $3p+p'$, where p is the total number of stories and p' is the number of DOFs of the ATMDs.

The state space formulation of the equation of motion of the actively controlled system is stated as follows:

$$\dot{\mathbf{z}} = \mathbf{A}\mathbf{z} + \mathbf{B}\mathbf{u} + \mathbf{H}\mathbf{f} \tag{1}$$

where $\mathbf{z}=[\mathbf{q}\ .\mathbf{q}]^{\mathbf{T}}$ is the state vector, $\mathbf{q}$ is the vector of generalized displacements of the structure–ATMD system, $\mathbf{A}$ is the system matrix, which contains the mass ($\mathbf{M_s}$), damping ($\mathbf{C_s}$), and stiffness ($\mathbf{K_s}$) matrices of the system, $\mathbf{f}$ is the vector of wind loads, $\mathbf{u}$ is the vector of control forces, $\mathbf{B}$ and $\mathbf{H}$ are the location matrices for the vectors $\mathbf{u}$ and $\mathbf{f}$, and a dot denotes time derivative.

The linear optimal control algorithm is used for the problem at hand, but the proposed optimization procedure could be readily applied to different control strategies. The linear quadratic performance index can be written as

$$J = \frac{1}{2}\int_0^\infty \left(\mathbf{z}^{\mathbf{T}}\mathbf{Q}\mathbf{z} + \mathbf{u}^{\mathbf{T}}\mathbf{R}\mathbf{u}\right)\mathrm{d}t \tag{2}$$

where $\mathbf{Q}$ and $\mathbf{R}$ are the weighting matrices of the state vector and the control forces vector, respectively. By application of the classic linear quadratic regulator (LQR) algorithm, the optimal gain matrix $\mathbf{K}$, which allows minimizing the performance index J in Equation (2), is computed and the feedback is calculated as $\mathbf{u}=-\mathbf{K}\mathbf{z}$.

DOI: 10.1002/stc

A limited number of stories are considered instrumented with three accelerometers per floor in order to measure the alongwind, acrosswind, and torsional accelerations. The output, $\mathbf{y}$, thus results in a linear combination of generalized nodal accelerations, as $\mathbf{y}=\mathbf{C_a}\ddot{\mathbf{q}}$, $\mathbf{C_a}$ being a convenient matrix that selects the monitored DOFs. Vector $\mathbf{y}$ can be rewritten in terms of state vector and control forces as

$$\mathbf{y}=\mathbf{Cz}+\mathbf{Du}+\mathbf{Hf}+\boldsymbol{\nu} \tag{3}$$

where

$$\begin{aligned}\mathbf{C} &= -\mathbf{C_a}\begin{bmatrix}\mathbf{M_s}^{-1}\mathbf{K_s} & \mathbf{M_s}^{-1}\mathbf{C_s}\end{bmatrix}\\ \mathbf{D} &= \mathbf{C_a}\mathbf{M_s}^{-1}\mathbf{B_0}\end{aligned} \tag{4}$$

and $\mathbf{v}$ is the vector of measurement noise.

To provide an estimate, $\hat{\mathbf{z}}$, of the state from the incomplete measurement set, a classic Kalman filter is used. Accordingly, the equation of the system with state observer can be written in terms of augmented state $\begin{bmatrix}\mathbf{z} & \hat{\mathbf{z}}\end{bmatrix}^T$ as

$$\begin{bmatrix}\dot{\mathbf{z}}\\ \dot{\hat{\mathbf{z}}}\end{bmatrix}=\begin{bmatrix}\mathbf{A} & -\mathbf{BK}\\ \mathbf{LC} & \mathbf{A}-\mathbf{BK}-\mathbf{LC}\end{bmatrix}\begin{bmatrix}\mathbf{z}\\ \hat{\mathbf{z}}\end{bmatrix}+\begin{bmatrix}\mathbf{Hf}\\ \mathbf{0}\end{bmatrix} \tag{5}$$

where $\mathbf{L}$ is the optimal Kalman gain matrix. In Equation (5), calculation of the feedback using the state estimate should be noticed.

The computation of the Kalman filter gain matrix $\mathbf{L}$ requires the hypothesis that both measurement and process vectors are realization of white Gaussian stochastic processes. Here, the measurement noise, $\mathbf{v}$, is assumed to satisfy such hypothesis, and its covariance matrix $\mathbf{R_n}=E[\mathbf{v}\mathbf{v}^t]$ is directly assigned. Although the wind process is non-Gaussian and nonwhite, the hypothesis of a white Gaussian wind process is here retained. Given the practical difficulty of directly measuring the cross-correlation of the wind forces $\mathbf{f}$, the covariance matrix $\mathbf{Q_n}=E[\mathbf{f}\mathbf{f}^t]$ may be obtained from simultaneous wind tunnel measurements of the pressure coefficients time histories.

3. OPTIMAL DESIGN OF THE CONTROL SYSTEM

In a general framework of incomplete number of actuators and sensors and limited power supply, the optimization problem is aimed at designing the hybrid control system, which gives the best structural response reduction, with due account given to the technological limitations of the actuators.

In order to minimize the computational effort, this goal is achieved through subsequent optimization steps:

1. Optimal configuration (number and position) of the array of ATMDs;
2. Optimal calibration of the parameters of the control system;
3. Optimal choice of the sensors' location.

Each step of the procedure is detailed in the following discussions.

3.1. Optimal configuration of the array of ATMDs

The first step of the optimization process consists in finding the optimal number and position of the ATMDs over the top floor of the building.

First of all, without loss of generality, a rectangular $(n \times m)$-dimensional grid is defined, which represents the potential positions of the ATMDs. The points are equally spaced over the two principal directions and are sufficiently far from the perimeter of the floor. Each point of the grid has coordinates defined with respect to a Cartesian reference system centered at the elastic center of the top floor of the building and having axes parallel to the building's principal directions.

The *design variables* for the problem at hand are the elements of a Boolean location matrix $\boldsymbol{\Psi}$, which stores $(n \times m)$ terms. Each term of $\boldsymbol{\Psi}$ is 1 or 0 depending on whether the ATMD is present or not in the corresponding position. The total number, n_{trial}, of ones contained in matrix $\boldsymbol{\Psi}$ is the number of ATMDs in the trial configuration.

DOI: 10.1002/stc

As each ATMD can move along both the x and y axes, the total number of DOFs of the system is $3p + 2n_{\text{trial}}$, where p is the stories number.

The optimal mass, stiffness, and damping of the generic ith ATMD are then adjusted to minimize the response of the translational and torsional modes of the structural system.

The total mass of the ATMDs, M_{ATMDs}, is set equal to a conveniently small percentage of the mass of the building M_{S}, for example, $\mu = M_{\text{ATMDs}}/M_{\text{S}}$ where μ is the total mass ratio of the ATMDs. Then, the mass of each ATMD is computed as a function of the distance from the elastic center. In particular, a portion $\Delta < 1$ of the total mass is assigned to the ATMDs, which are comprised within a certain distance $d_{\max}$ from the elastic center, while the $1 - \Delta$ left portion is assigned to the ATMDs located at a distance greater than $d_{\max}$. If d_i is the distance of the ith ATMD from the elastic center, this condition gives

$$\begin{aligned} \text{Central masses}: &\quad \sum_{i=1,\ldots,n_{\text{trial}}} m_{\text{ATMD},i} \cdot \delta_i^{d\max} = \Delta\mu M_{\text{S}} \\ \text{Eccentric masses}: &\quad \sum_{i=1,\ldots,n_{\text{trial}}} m_{\text{ATMD},i} \cdot \left(1 - \delta_i^{d\max}\right) = (1-\Delta)\mu M_{\text{S}} \end{aligned} \tag{6}$$

where $\delta_i^{d\max} = \begin{cases} 1 \text{ if } d_i \leqslant d_{\max} \\ 0 \text{ if } d_i > d_{\max} \end{cases}$ and $m_{\text{ATMD},i}$ is the mass of the ith ATMD.

Once the masses of the devices are known, their stiffness characteristics can be obtained by tuning the ATMDs to the first three modes of the building. The stiffnesses of the central ATMDs are computed using the first two flexural circular frequencies $\omega_{\text{S},1}$, $\omega_{\text{S},2}$, and the stiffnesses of the eccentric ATMDs are computed using the first torsional circular frequency $\omega_{\text{S},3}$:

$$k_{\text{ATMD},i} = m_{\text{ATMD},i}\alpha_{\text{opt},i}^2\omega_{\text{S},j}^2 \qquad i = 1, \ldots, n_{\text{trial}} \qquad j = 1, 2, 3 \tag{7}$$

where $\alpha_{\text{opt},i} = \frac{\omega_{\text{ATMD},i}}{\omega_{\text{S},i}} = \frac{\sqrt{(1+\mu_i/2)}}{1+\mu_i}$ is the optimal tuning ratio according to Warburton [19], $\mu_i = m_{\text{ATMD},i}/M_{\text{S},i}$ is the mass ratio of the ith ATMD and $M_{\text{S},i}$ is the ith modal mass of the structure.

The damping coefficient of the ith ATMD is computed using the following expression:

$$c_{\text{ATMD}i} = 2m_{\text{ATMD}i}\gamma_{\text{opt}}^i\omega_{\text{S}}^j \qquad i = 1, \ldots, n_{\text{trial}} \qquad j = 1, 2, 3 \tag{8}$$

where $\gamma_{\text{opt}}^i = \sqrt{\frac{\mu_i(1+3\mu_i/4)}{(1+\mu_i)(1+\mu_i/2)}}$ is the optimal damping ratio according to Warburton [19].

In Equation (8), the circular frequencies of the flexural modes $\omega_{\text{S},1}, \omega_{\text{S},2}$ are used for the central ATMDs, while the circular frequency of the torsional mode $\omega_{\text{S},3}$ is used for the eccentric ATMDs.

The *objective function*, $f_1(\boldsymbol{\Psi})$, is a function of the position of the ATMDs, that is, of the location matrix $\boldsymbol{\Psi}$:

$$f_1(\boldsymbol{\Psi}) = G_1(\boldsymbol{\Psi}) + P_1(\boldsymbol{\Psi}) \tag{9}$$

In the following discussions, $G_1(\boldsymbol{\Psi})$ is a combination of the translational and rotational response components at a control point of the building. The function $P_1(\boldsymbol{\Psi})$ is a penalty term that is added to the objective function, in order to discard the solution, when the constraints are violated.

The *constraints* to the problem are limitations on the mass, stiffness, and damping of the ATMDs in order to make the control system technically feasible. Moreover, an additional constraint is included in order to force the coincidence of the elastic centers of the structure and the control system. In this way, any disturbance due to the ATMDs in presence of purely flexural motions is avoided.

In the problem at hand, the objective function cannot be written as an explicit function of the design variables. As it is cumbersome to numerically compute the derivatives of the objective function, a random search algorithm is used instead of gradient-based methods [25]. In particular, in this and in the following steps of the optimization procedure, a classic genetic algorithm is adopted, whose effectiveness and numerical efficiency are widely recognized in the literature [26,27].

DOI: 10.1002/stc

3.2. Optimal calibration of the LQR performance index

The optimal calibration of the weight matrices **R** and **Q** applied to the state vector and the control forces in the LQR performance index, Equation (2), is also achieved through an optimization procedure.

The matrix **R** is assumed to be equal to the product between the identity matrix **I** and a coefficient φ_1, while the matrix **Q** is the product between the identity matrix **I** and a set of coefficients $\varphi_2,\ldots,\varphi_k$, where the vector $\mathbf{\Phi} = [\varphi_1,\ldots,\varphi_k]^{\mathrm{T}}$ stores the *design variables* of this subproblem. In order to reduce the computational effort, a lower and an upper bounds are imposed to the design variables:

$$\varphi_{i,\min} \leqslant \varphi_i \leqslant \varphi_{i,\max} \qquad i = 1,\ldots,k \tag{10}$$

where the bounds $\varphi_{i,\min}$ and $\varphi_{i,\max}$ are assigned on the basis of a preliminary sensitivity analysis.

In this optimization subproblem, the objective function, $f_2(\mathbf{\Phi})$, to be minimized is defined as

$$f_2(\mathbf{\Phi}) = G_2(\mathbf{\Phi}) + P_2(\mathbf{\Phi}) \tag{11}$$

where $G_2(\mathbf{\Phi}) = \sum_{i=x,y,\theta} \sigma_i^{\mathrm{HYB}}(\mathbf{\Phi}) / \sum_{i=x,y,\theta} \sigma_i^{\mathrm{PASS}}$ and $P_2(\mathbf{\Phi})$ is the penalty function. In $G_2(\mathbf{\Phi})$, $\sum_{i=x,y,\theta} \sigma_i^{\mathrm{HYB}}(\mathbf{\Phi})$ is the sum of the standard deviations of the accelerations of the elastic center of the top floor of the hybridly controlled system, and $\sum_{i=x,y,\theta} \sigma_i^{\mathrm{PASS}}$ is the sum of the standard deviations of the accelerations of the top floor of the passively controlled system.

The nonlinear constraints to the subproblem are the following:

$$\begin{cases} u_j \leqslant u_{\max} \\ q_{\mathrm{TMD},j} \leqslant q_{\mathrm{TMD},\max} \end{cases} \quad (j = 1,\ldots,2n_{\mathrm{trial}}) \tag{12}$$

where u_j are the control forces, $u_{\max}$ is the upper bound of the control forces, $q_{\mathrm{TMD},j}$ are the strokes of the ATMDs, and $q_{\mathrm{TMD},\max}$ is the upper bound of the ATMDs strokes. The upper bounds $u_{\max}$ and $q_{\mathrm{TMD},\max}$ depend on the technical characteristics of the selected control devices. To keep into account the constraints, a penalty function $P_2(\mathbf{\Phi})$ is added to the objective function when the constraints are violated in order to discard the solution.

3.3. Optimal choice of the sensors' location

The third phase of the optimization procedure leads to the optimization of the sensors locations along the height of the building.

In this optimization subproblem, the *multi-objective function*, $f_3(\mathbf{\Omega})$, to be minimized is

$$f_3(\mathbf{\Omega}) = G_3(\mathbf{\Omega}) + P_3(\mathbf{\Omega}) = \sum_{i=x,y,\theta} \sigma_i^{\mathrm{OBS}}(\mathbf{\Omega}) / \sum_{i=x,y,\theta} \sigma_i^{\mathrm{HYB}}(\mathbf{\Omega}) + P_3(\mathbf{\Omega}) \tag{13}$$

where the *design variable* $\mathbf{\Omega}$ is a $(t \times 1)$ location vector with t number of instrumented floors, $\sum_{i=x,y,\theta} \sigma_i^{\mathrm{OBS}}(\mathbf{\Omega})$ is the sum of the standard deviations of the accelerations along the x and y directions and the rotational acceleration of the hybridly controlled system instrumented with a limited number of sensors, and $\sum_{i=x,y,\theta} \sigma_i^{\mathrm{HYB}}(\mathbf{\Omega})$ is the sum of the standard deviations of the accelerations of the ideal hybridly controlled system, that is, the system with full state knowledge.

The location vector $\mathbf{\Omega}$ contains numbers from 1 to p, with p equal to the total number of stories, to identify which are the instrumented floors:

$$1 \leqslant \Omega_i \leqslant p \qquad i = 1,\ldots,t \tag{14}$$

Three accelerometers are arranged over each instrumented floor to measure accelerations along the three DOFs.

The nonlinear constraints to the subproblem are expressed by Equation (12), as in the previous substep.

DOI: 10.1002/stc

4. NUMERICAL EXAMPLE

4.1. Description of the structure

The proposed procedure is applied to a 60-story square tall building with dimensions: $30 \times 30 \times 180$ m. The structure was designed, according to the structural Eurocodes, for wind loads corresponding to a mean reference wind speed of 30 m/s (10-min gust) at 10 m height in open terrain and a 50-year mean recurrence interval.

The structure is made of steel frames with a central core and systems of bracings in both the principal directions. A grid of 25 columns equally spaced in both the principal directions is arranged over the plan of the structure. Columns are made of square tubes with side length and thickness varying along the height of the building. Beams are I-flange, and diagonals are rectangular tubes with dimensions varying over the floors. The central core is made of columns, beams, and X bracings in both directions. Three additional systems of bracings are located over the perimeter of the structure every 20 floors. Floors are reinforced concrete slabs, 0.2 m thick, capable of warranting a rigid in-plane behavior. In Table I are reported the modal characteristics of the system.

The structure is modeled as a simplified dynamic system having three DOFs for each floor obtained by static condensation from a detailed finite element model of the structure (Figure 1). Mass, stiffness, and damping matrices of the simplified structural model are available on the web [28] for researchers that would like to compare their results with those obtained using the procedure proposed in this paper.

4.2. Wind load modeling

The forcing functions representing the wind load are obtained from synchronous wind tunnel pressure measurements. The experimental tests were carried out in the boundary-layer wind tunnel operated by CRIACIV (Inter-university Research Center on Buildings Aerodynamic and Wind Engineering) in Prato, Italy. The rigid 1/500 scale model of the building, having a total height of 36 cm, was instrumented with 120 pressure taps, 30 for each side. In particular, for each side of the structure, five taps were located at the following heights: 4.15, 12.9, 19.5, 24.4, 29.3, and 34 cm. The sampling frequency was 250 Hz, and the duration of the records was 30 s. Tests were carried out in suburban terrain conditions. In particular, the exponent of the mean wind profile was $\alpha = 0.22$, the mean wind speed at the top of the model was 18.3 m/s, and the turbulence intensity at the same height was 7%. In Figure 2 is shown the time history of the pressure coefficient measured at the center of the windward side at the height of 24.4 cm, corresponding to a real height of 122 m. Its mean value is 0.85, and its standard deviation is 0.145.

To make the pressure time histories measured in the wind tunnel representative of the real phenomenon, the similitude criterion on the reduced frequency is respected:

$$\frac{n_m \cdot D_m}{V_m} = \frac{n_p \cdot D_p}{V_p} \tag{15}$$

where $n = 1/\delta t$ is the frequency of the forcing function, V is the mean wind speed at height H, and D is the side length. The subscript m refers to the model while the subscript p to the prototype. The time interval $\delta t = 1/n_p$ used for the integration is $\delta t = D_p \cdot V_m / D_m \cdot V_p \cdot n_m$ that is a function of the wind speed. As $D_p/D_m = 500$, $V_m = 18.3$ m/s, $V_p = 47$ m/s, and $n_m = 250$ Hz, the time interval used is 0.778 s. Then, time histories have been re-sampled dividing each time interval in five equal parts. The total duration of the pressure coefficients' time histories in the prototype scale is about 5800 s.

Table I. Modal characteristics of the structure.

Mode	Frequency (Hz)	Modal mass (kg)	Modal damping
1—Bending *X* (BX1)	0.208	1.039e7	0.01
2—Bending *Y* (BY1)	0.215	1.081e7	0.01
3—Torsion (T1)	0.287	2.331e9	0.01
4—Torsion (T2)	0.610	1.991e9	0.01
5—Bending *X* (BX2)	0.637	9.653e6	0.01
6—Bending *Y* (BY2)	0.640	9.607e6	0.01

DOI: 10.1002/stc

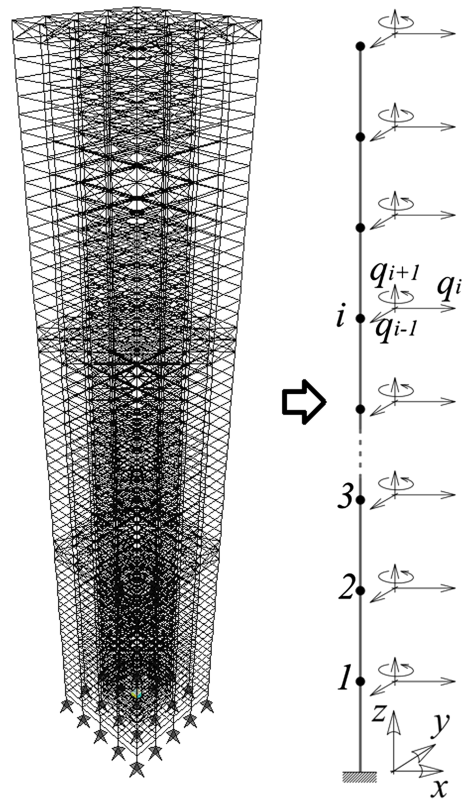

Figure 1. Finite element model of the analyzed structure and corresponding simplified dynamic system with three DOFs for each floor.

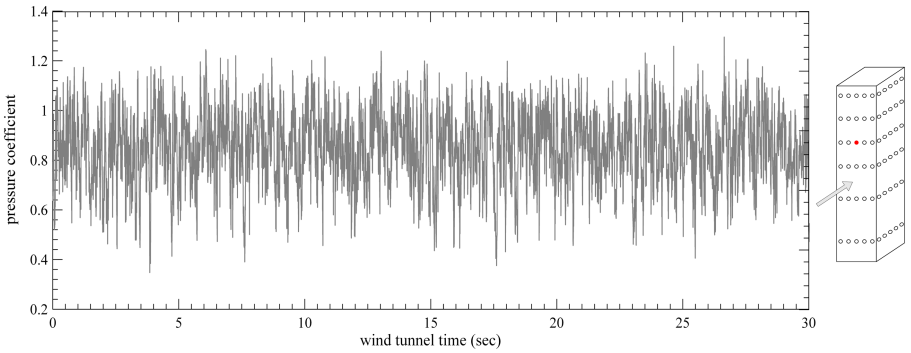

Figure 2. Sample time history of a pressure coefficient measured in the wind tunnel (the pressure tap is indicated in the sketch of the scaled-down building model shown on the right of the plot).

For structural response analysis, the measured pressure coefficients' time histories are integrated over the surface of the building, yielding the resultant wind force time histories in x and y direction as well as the torsional moments at the elastic center of each floor. These quantities are available to other researchers upon request to the authors.

4.3. Results

4.3.1. Optimal ATMDs' positioning. The first step of the optimization process consists in finding the optimal number and position of the ATMDs. With this aim, a 5×5 square grid is defined, which represents all the possible ATMDs' positions (Figure 3) over the top floor of the building. In particular, the 25 feasible positions are equally spaced along both the principal directions. The

DOI: 10.1002/stc

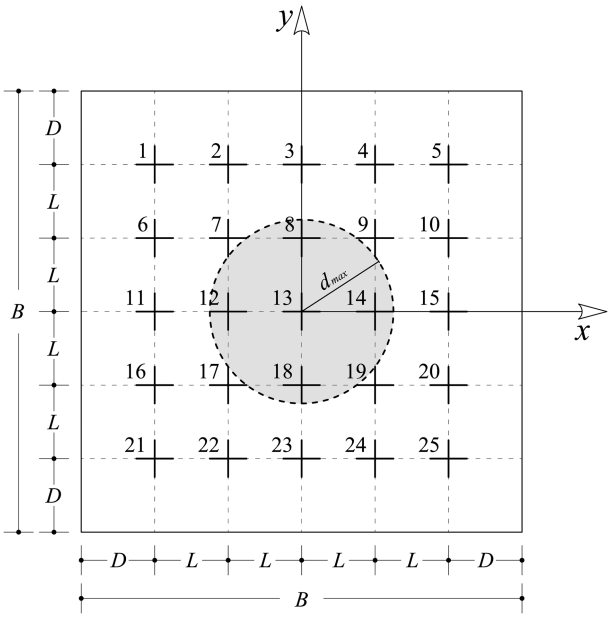

Figure 3. Possible active tuned mass dampers' locations over the top floor.

distance between one point to another is $L = 5$ m, and the distance of the perimetrical points from the edge of the top floor is $D = 5$ m. As explained in Section 3, the feasible points are divided into two categories: the central ATMDs are those for which the condition $d_i < d_{\max}$ applies, and the eccentric ATMDs are those for which the condition $d_i > d_{\max}$ applies, where d_i is the distance of the ith feasible point from the elastic center of the top floor and $d_{\max}$ is a conventional maximum distance. The *design variables* for the problem at hand are the elements of a Boolean location matrix $\mathbf{\Psi}$, which stores 25 terms. Each term of $\mathbf{\Psi}$ is 1 or 0 depending on whether the ATMD is present or not in the corresponding position.

Several *objective functions* are defined, which are linear combinations of some terms:

$$f_1^a(\mathbf{\Psi}) = \frac{\sum_{i=x,y,\theta} C_i \sigma_i^{\mathrm{PASS}}(\mathbf{\Psi})}{\sum_{i=x,y,\theta} C_i \sigma_i{}^{\mathrm{UNC}}(\mathbf{\Psi})} + P_1(\mathbf{\Psi}) \tag{16}$$

$$f_1^b(\mathbf{\Psi}) = \frac{\sum_{i=\theta} \sigma_i^{\mathrm{PASS}}(\mathbf{\Psi})}{\sum_{i=\theta} \sigma_i{}^{\mathrm{UNC}}(\mathbf{\Psi})} + P_1(\mathbf{\Psi}) \tag{17}$$

$$f_1^c(\mathbf{\Psi}) = \frac{\sum_{i=x,y} C_i \sigma_i^{\mathrm{PASS}}(\mathbf{\Psi})}{\sum_{i=x,y} C_i \sigma_i{}^{\mathrm{UNC}}(\mathbf{\Psi})} + P_1(\mathbf{\Psi}) \tag{18}$$

$$f_1^d(\mathbf{\Psi}) = \frac{\sum_{i=x,y,\theta} C_i \sigma_i^{\mathrm{PASS}}(\mathbf{\Psi})}{\sum_{i=x,y,\theta} C_i \sigma_i{}^{\mathrm{UNC}}(\mathbf{\Psi})} + \frac{1}{n_{\mathrm{trial}}}(\mathbf{\Psi}) + P_1(\mathbf{\Psi}) \tag{19}$$

In Equation (16), the first term is the ratio between the weighted sum of the standard deviations, $\sum_{i=x,y,\theta} C_i \sigma_i^{\mathrm{PASS}}(\mathbf{\Psi})$, of the accelerations along x, y, and around z obtained with the passively controlled system and the sum of the standard deviations of the same accelerations $\sum_{i=x,y,\theta} \sigma_i{}^{\mathrm{UNC}}(\mathbf{\Psi})$ obtained with the uncontrolled system. In order to avoid additional torsional moments to the structure, the penalty $P_1(\mathbf{\Psi})$ is added when there is no coincidence of the elastic centers of the structure, G_s, and the control system, G_c, as stated in Equation (20):

DOI: 10.1002/stc

$$\begin{aligned} P(\boldsymbol{\Psi}) &= 0 \quad \textit{if } G_s \equiv G_c \\ P(\boldsymbol{\Psi}) &= 10 \quad \textit{if } G_s \neq G_c \end{aligned} \tag{20}$$

Equations (17) and (18) express the same objective function as in Equation (16) in which, respectively, the rotations around z or the sum of the two translations along x and y are considered. Equation (19) contains an additional term with respect to Equation (16) that is proportional to the inverse of the number of ATMDs. This term decreases when the number of ATMDs increases and tends to diminish the single masses of the ATMDs.

The weights of the generalized displacements in this specific applications are $C_i = 1$, $i = 1,2,3$ but may be varied to give different importance to the minimization of the components of the response.

In Table II are summarized the parameters chosen for the implementation of the genetic algorithm for the problem at hand.

As an example, in Figure 4 is shown the evolution of the best and mean value of the objective function $f_1^a(\boldsymbol{\Psi})$ during the optimization process. It may be noted the quick convergence of the optimization algorithm.

In Table III are reported the results of the optimization of the ATMD's position.

Results summarized in Table III show that a central mass is effective in reducing the translational response, while two or four symmetric masses located at the corners of the grid minimize the torsional response.

4.3.2. Optimal LQR index. The second step of the optimization procedure is the calibration of the LQR weighting coefficients, that is, matrices **Q** and **R** in Equation (2).

The comparison between the modal characteristics of the uncontrolled structure and the passively controlled structure, optimized as in Section 4.3.1 by using Equation (16), are summarized in Table IV.

In this case, the choice of the control forces and the maximum extensions of the strokes of the ATMD are the main control constraints to be satisfied. Indeed, in principle, there would be essentially no upper limit to the control effectiveness of the system if these constraints were not accounted for. Nevertheless, the obvious counterparts of a large control effectiveness are large strokes extensions and large control forces. Hence, the aforementioned physical limitations dictate, in practice, the

Table II. Parameters for the genetic algorithm.

Parameter	Value
Population size	100
Maximum iterations number	100
Function tolerance	10^{-6}
Elite count	2
Crossover fraction	0.8
Migration fraction	0.2

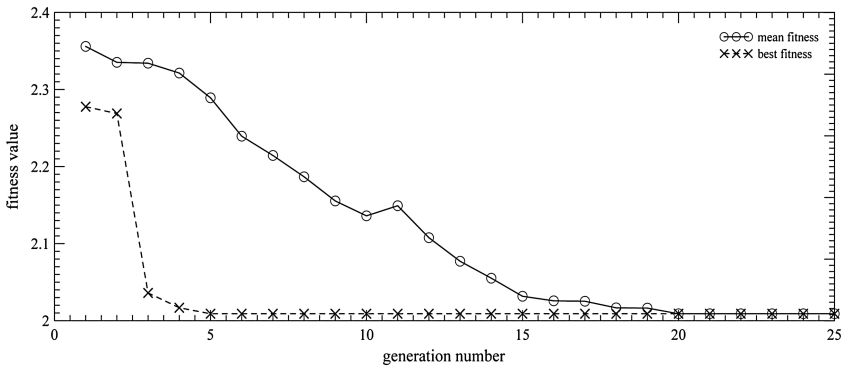

Figure 4. Evolution of the best and mean value of the objective function $f_1^a(\boldsymbol{\Psi})$.

DOI: 10.1002/stc

Table III. Results of the optimization of the active tuned mass dampers' position.

Objective function	Optimal configuration	Minimum value of the objective function	Generations required
$f_1^a(\mathbf{\Psi})$	1–13–25	2.009	19
$f_1^b(\mathbf{\Psi})$	1–25	0.559	14
$f_1^c(\mathbf{\Psi})$	3–11–13–15–23	1.307	14
$f_1^d(\mathbf{\Psi})$	1–5–8–12–14–18–21–23	2.207	16

Table IV. Comparison between the modal characteristics of the uncontrolled structure and the passively controlled structure.

Mode	Frequency (Hz) uncontrolled	Frequency (Hz) passively controlled
1	0.208	0.195
2	0.215	0.202
3	0.287	0.220

Table V. Constraints of the hybrid control system.

Maximum control force (kN)	Maximum stroke (m)
u	q_{ATMD}
1000	2.5

Table VI. Lower and upper bounds for the design variables.

Design variable	φ_1	φ_2	φ_3	φ_4	φ_5	φ_6	φ_7	φ_8	φ_9
Bounds	15–25	1–15	0–1	0–1	0–1	0–1	0–1	0–1	0–1
Optimal value	21.4	14.92	0.03	0.105	0.036	0.182	0.653	0.143	0.01

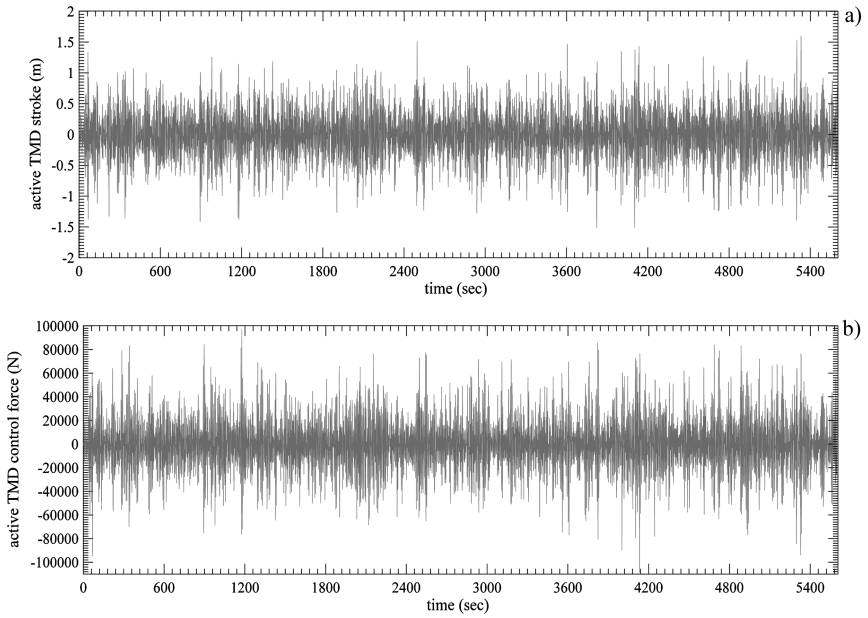

Figure 5. Stroke of the central active tuned mass damper (TMD) along the y direction and corresponding control force.

DOI: 10.1002/stc

maximum achievable control effectiveness. The control constraints considered in this work are summarized in Table V.

The matrices **R** and **Q** of the LQR performance index are defined as follows:

$$\mathbf{R}(\mathbf{\Phi}) = 10^{-\varphi_1} \cdot \mathbf{I}_1 \tag{21}$$

$$\mathbf{Q}(\mathbf{\Phi}) = \mathbf{q}(\mathbf{\Phi}) \cdot \mathbf{I}_2 \tag{22}$$

where $\mathbf{I_1}$ and $\mathbf{I_2}$ are identity matrices and $\mathbf{q}(\mathbf{\Phi})$ is a matrix that stores at the proper positions the coefficients $\varphi_2, \ldots, \varphi_9$ of the design variable vector $\mathbf{\Phi}$.

In this numerical example, the design variables are the following:

φ_1: exponent of the coefficient that multiplies matrix **R**
φ_2: weighting coefficient of the structural rotations in matrix **Q**
$\varphi_3, \ldots, \varphi_8$: weighting coefficients of the ATMDs' displacements in matrix **Q**
φ_9: weighting coefficients of the ATMDs' velocities in matrix **Q**.

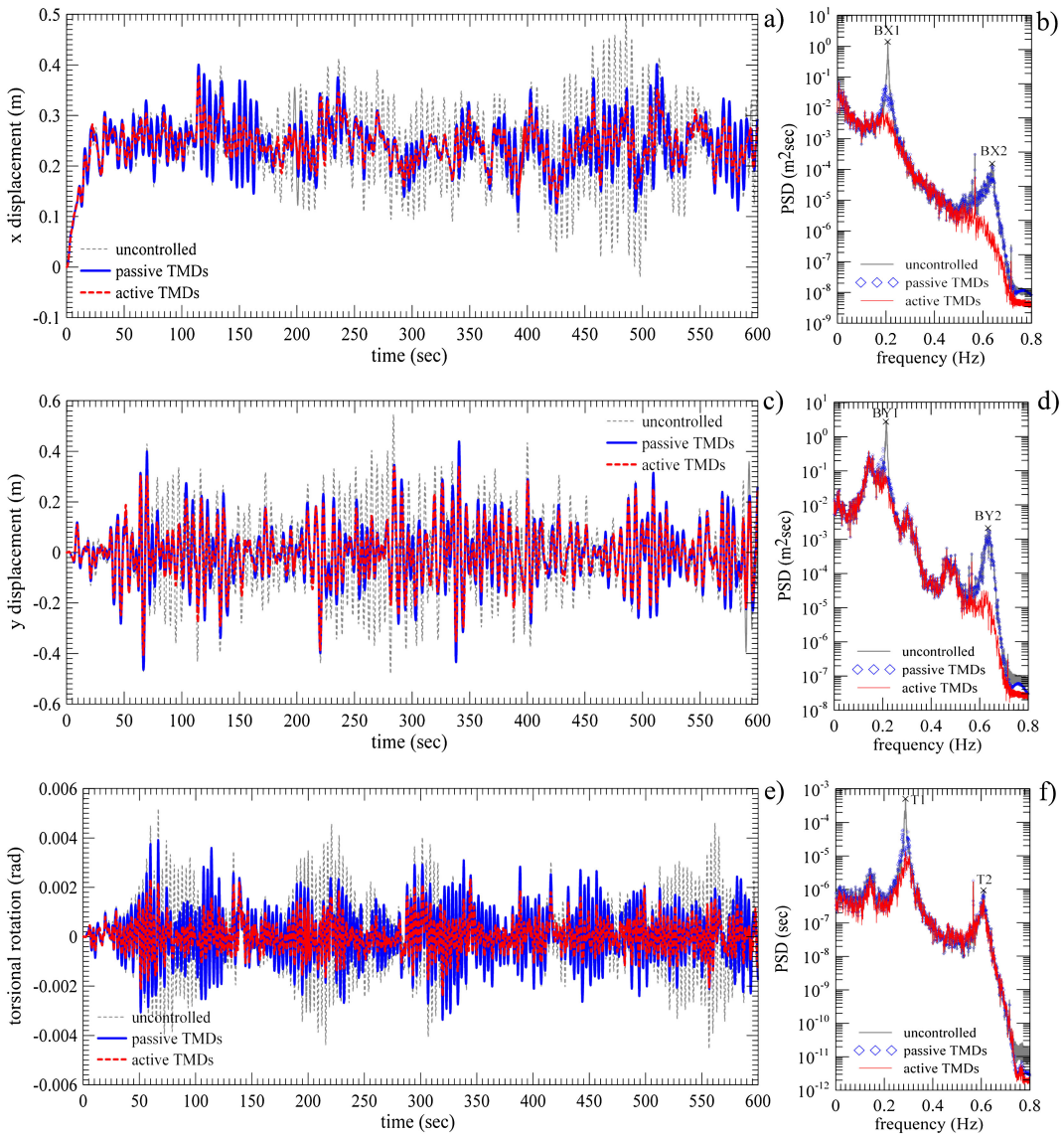

Figure 6. Displacements in the *x* (a) and *y* (c) directions and rotations (e) at the top floor and corresponding power spectral densities (b, d, f) for the uncontrolled, passively controlled and actively controlled systems.

DOI: 10.1002/stc

A preliminary analysis provides proper bounds for the design variables, as summarized in Table VI. In the same Table VI are reported the optimal values of the design variables obtained with the optimization procedure described in Section 3.2 and with the parameters of the genetic algorithm summarized in Table II.

In Figure 5 are reported the stroke of the central ATMD along the *y* direction and the corresponding control force. It can be noted that in the optimized control system, constraints are never exceeded.

In Figure 6 are shown the time histories of the *x* and *y* components of the displacements and the rotation at the top floor for the cases of uncontrolled system, passively controlled system and hybridly controlled system. The corresponding power spectral densities (PSDs) are also shown in Figure 6. In order to allow the visual identification of the different response quantities, 10-min responses are shown in Figure 6. Instead, the PSDs of the displacements and rotation are computed using the full-length time histories (5800 s long) of the response.

Maximum values and standard deviations of the generalized displacements of the top floor are also summarized in Table VII, while Figure 7 shows the variations of the maximum generalized displacements along the height of the building. The results presented in Table VII and in Figure 7 are referred to the full-length time histories of the response.

From the presented results, it can be noticed that the passive solution is already quite effective in reducing the structural response. In particular, as expected, it is effective in significantly reducing the peaks of the lowest modes. However, passive TMDs are known to be quite sensitive to frequency mistuning, which is almost unavoidable in practice. To overcome this drawback, one possible solution is to upgrade towards the hybrid approach. Moreover, as shown in Figures 6, 7 and in Table VII, the hybrid control system is sensibly more effective than the passive TMDs in mitigating the torsional response, and it also allows to reduce the peaks of the higher modes.

Table VII. Structural response at the top of the building for the uncontrolled, passively controlled and actively controlled systems.

Response type	Uncontrolled	Passive TMDs	Active TMDs
Max displacement *X* (m)	0.513	0.414	0.382
Max displacement *Y* (m)	0.640	0.517	0.450
Max rotation (rad)	6.6e-3	5.9e-3	3.2e-3
Std displacement *X* (m)	0.081	0.049	0.039
Std displacement *Y* (m)	0.164	0.119	0.105
Std rotation (rad)	1.7e-3	1.2e-3	7.0e-4

TMDs, tuned mass dampers.

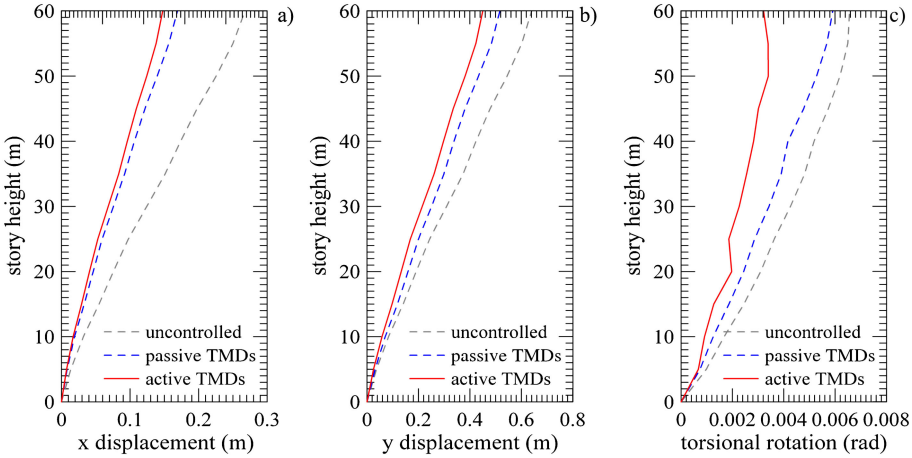

Figure 7. Variation along the height of the maximum generalized displacements for the uncontrolled, passively controlled and actively controlled systems.

DOI: 10.1002/stc

Table VIII. Reduction of the maximum response obtained considering the hybrid control with and without state observer with respect to the uncontrolled case.

Control type	Displ. X (%)	Displ. Y (%)	Rotation (%)	Acc. X (%)	Acc. Y (%)	Rotational acc. (%)
Hybrid without state observer	44.7	29.6	11.5	53.2	50.1	10.5
Hybrid with state observer	44.9	29.8	10.2	51.7	48.4	9.8

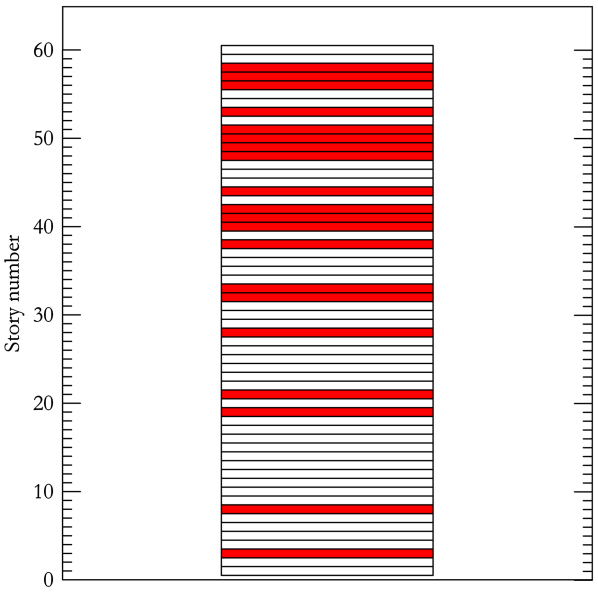

Figure 8. Optimal position of the accelerometers along the building's height.

4.3.3. Optimal sensors positioning. The final step of the proposed design methodology is the optimization of the position of the monitoring sensors by applying the procedure presented in Section 3.3.

A number of 20 instrumented floors are considered in this application. It is observed that, already with a relatively small number of sensors, the effectiveness of the control system is essentially similar to the ideal case. On this respect, in Table VIII are summarized the reductions of the maximum response in terms of displacements and accelerations obtained considering the hybrid control with and without state observer with respect to the uncontrolled case.

The optimization leads to the results presented in Figure 8. It should be noticed that, in the optimal solution, sensors are concentrated around floors 20 and 40, where the presence of systems of bracings significantly influences the deformed shape of the building, and in the upper part of the structure, where the response components have the highest values.

5. CONCLUSIONS

In this paper, a comprehensive procedure is developed for the optimization of a hybrid control system for tall buildings subjected to wind load. The control system is made of an array of ATMDs and is conceived to mitigate the flexural and torsional responses. The feedback information necessary to compute the control forces is provided by a limited number of accelerometers arranged over the building's height. The chosen control algorithm is the classic LQR complemented with a Kalman observer for state tracking using acceleration measurements.

DOI: 10.1002/stc

In order to minimize the computational effort, the optimization is achieved through subsequent substeps: (1) evaluation of the optimal configuration of the ATMDs' array; (2) optimal calibration of the parameters of the control system; and (3) optimal choice of the sensors' location.

The main advantage of this approach is that it does not require approximations on the characteristics of the wind-induced actions and of the dynamic system under investigation and provides automatically the optimal design of all the components of the control system.

From the application to a case study, it has been observed that the optimization procedure is capable to find the most effective configuration of the array of ATMDs, which, working as passive system, minimizes the flexural and torsional response.

The improvement of control effectiveness achieved by means of the hybrid approach, for realistic values of the control constraints, with respect to the optimal passive case should be regarded as substantial in the sense that the hybrid control solution does not suffer from mistuning issues and yields a significant improvement in the mitigation of the torsional response.

The optimal calibration of the parameters of the LQR control algorithm is performed in order to obtain a solution that respects the physical limitations of the system in terms of maximum strokes and maximum control forces.

The classic Kalman state observer is seen to be quite effective for the chosen application, and the genetic algorithm showed to be fast in providing the optimal set of design variables and stable with respect to the initial guess population.

ACKNOWLEDGEMENTS

The authors gratefully acknowledge the financial support of the 'Cassa di Risparmio' Foundation, which partially funded this study through the project 'Development of active control systems for the response mitigation under seismic excitation' (project code 2010.011.0490).

REFERENCES

1. Chu SY, Soong TT, Reinhorn AM. *Active, Hybrid, and Semi-active Structural Control: A Design and Implementation Handbook*. Wiley: Hoboken, NJ, 2005.
2. Lin CC, Ueng JM, Huang TC. Seismic response reduction of irregular buildings using passive tuned mass dampers. *Engineering Structures* 1999; **22**:513–524.
3. Hoang N, Fujino Y, Warnitchai P. Optimal tuned mass damper for seismic applications and practical design formulas. *Engineering Structures* 2008; **30**(3):707–715.
4. Jangid RS, Datta TK. Performance of multiple tuned mass dampers for torsionally coupled system. *Earthquake Engineering and Structural Dynamics* 1997; **26**:307–317.
5. Varadarajan N, Nagarajaiah S. Wind response control of building with variable stiffness tuned mass damper using EMD/HT. *Journal of Engineering Mechanics* 2004; **130**(4):451–458.
6. Casciati F, Giuliano F. Performance of multi-TMD in the towers of suspension bridges. *Journal of Vibration and Control* 2009; **15**(6):821–847.
7. Matta E, De Stefano A. Robust design of mass-uncertain rolling-pendulum TMDs for the seismic protection of buildings. *Mechanical Systems and Signal Processing* 2009; **23**(1):127–147.
8. Ubertini F. Prevention of suspension bridge flutter using multiple tuned mass dampers. *Wind and Structures* 2010; **13**(3):235–256.
9. Chakraborty S, Roy BK. Reliability based optimum design of tuned mass damper in seismic vibration control of structures with bounded uncertain parameters. *Probabilistic Engineering Mechanics* 2011; **26**(2):215–221.
10. Mohtat A, Dehghan-Niri E. Generalized framework for robust design of tuned mass damper systems. *Journal of Sound and Vibration* 2011; **330**(5):902–922.
11. Casciati S, Chen ZC. An active mass damper system for structural control using real-time wireless sensors. *Structural Control and Health Monitoring* 2012; DOI: 10.1002/stc.1485
12. Ankireddi S, Yang HTY. Simple ATMD control methodology for tall buildings subject to wind loads. *Journal of Structural Engineering* 1996; **122**(1):83–91.
13. Li C, Zhang J. Investigations of vibration control of tall buildings under wind loads using active tuned mass damper. *Journal of Earthquake Engineering and Engineering Vibration* 2007; **27**(5):160–165.
14. Yan N, Wang CM, Balendra T. Optimal damper characteristics of ATMD for buildings under wind loads. *Journal of Structural Engineering* 1999; **125**(12):1376–1383.
15. Ahlawat AS, Ramaswamy A. Multiobjective optimal fuzzy logic control system for response control of wind-excited tall buildings. *Journal of Engineering Mechanics* 2004; **130**(4):524–530.
16. Li C, Li J, Qu Y. An optimum design methodology of active tuned mass damper for asymmetric structures. *Mechanical Systems and Signal Processing* 2010; **24**(3):746–765.
17. Li C, Xiong X. Estimation of active multiple tuned mass dampers for asymmetric structures. *Structural Engineering and Mechanics* 2008; **29**(5):505–53.
18. Li C, Han B, Zhang J, Qu Y, Li J. Active multiple tuned mass dampers for reduction of undesirable oscillations of structures under wind loads. *International Journal of Structural Stability and Dynamics* 2009; **9**(1):127–149.

DOI: 10.1002/stc

19. Warburton GB. Optimum absorber parameters for various combinations of response and excitation parameters. *Earthquake Engineering and Structural Dynamics* 1982; **10**(3):381–401.
20. Chang CC. Mass dampers and their optimal designs for building vibration control. *Engineering Structures* 1999; **21**:454–463.
21. Lu X, Chen J. Parameter optimization and structural design of tuned mass damper for shanghai centre tower. *Structural Design of Tall and Special Buildings* 2011; **20**(4):453–471.
22. Marano CG, Greco R. Optimization criteria for tuned mass dampers for structural vibration control under stochastic excitation. *Journal of Vibration and Control* 2011; **17**(5):679–688.
23. Materazzi AL, Ubertini F. Robust structural control with system constraints. *Structural Control and Health Monitoring* 2012; **19**:472–490.
24. Cha YJ, Raich A, Barroso L, Agrawal A. Optimal placement of active control devices and sensors in frame structures using multi-objective genetic algorithms. *Structural Control and Health Monitoring* 2011; DOI: 10.1002/stc.468
25. Venanzi I, Materazzi AL. Multi-objective optimization of wind-excited structures. *Engineering Structures* 2007; **99**(6):983–990.
26. Manoharana S, Shanmuganathan A. A comparison of search mechanisms for structural optimization. *Computer & Structures* 1999; **73**:363–372.
27. Woon SY, Querin OM, Steven GP. Structural application of a shape optimization method based on a genetic algorithm. *Structural and Multidisciplinary Optimization* 2001; **22**:57–64.
28. http://www.strutture.unipg.it/materazzi/Benchmark_tall_building_control/Tall_building.zip, 2012.

DOI: 10.1002/stc